

Iromycins from *Streptomyces* sp. and from synthesis: New inhibitors of the mitochondrial electron transport chain

Frank Surup,^a Heydar Shojaei,^a Paultheo von Zezschwitz,^{a,*}
Brigitte Kunze^{b,*} and Stephanie Grond^{a,*}

^a*Institute of Organic and Biomolecular Chemistry, Georg-August-Universität Göttingen, Tammannstrasse 2,
37077 Göttingen, Germany*

^b*Research Group of Microbial Communication, Helmholtz Centre for Infection Research, Inhoffenstrasse 7,
38124 Braunschweig, Germany*

Received 9 July 2007; revised 31 October 2007; accepted 7 November 2007

Available online 13 November 2007

Abstract—Two new α -pyridone metabolites, iromycins E and F, were isolated from cultures of strain *Streptomyces* sp. Dra 17, thus expanding the recently discovered iromycin family. The inhibitory potential on the mitochondrial respiratory chain was examined and revealed that iromycin metabolites block NADH oxidation in beef heart submitochondrial particles with different efficacy, yet remarkably show only very low cytotoxicity. Difference spectroscopic studies indicated that iromycins inhibit the electron transport at the site of complex I (NADH-ubiquinone oxidoreductase). Derivatives of the natural products were semisynthetically prepared and provided detailed insights into structure–activity relationships. Drawn from these results, there are strong similarities with the piericidins, which are among the most potent complex I inhibitors of the mitochondrial electron transport chain. Furthermore, total synthesis afforded new analogues, and the non-natural iromycin S (IC_{50} = 58 ng/mL) emerged as the most active compound, thus opening avenues of future studies with the iromycins as new valuable biochemical tools.

© 2007 Elsevier Ltd. All rights reserved.

1. Introduction

The respiratory chain (electron transport chain) with its particular functional complexes in the lipid bilayer membranes is one of the most important biochemical cascade reactions in the energy supply of all living organisms.¹ The enzymes, which mediate electron transfer and ATP synthesis in a sequence of redox reactions of the oxidative phosphorylation, are exclusively located in mitochondria or bacterial membranes, respectively. The impairment of this energy metabolism is associated with dysfunction of cells or cell death.

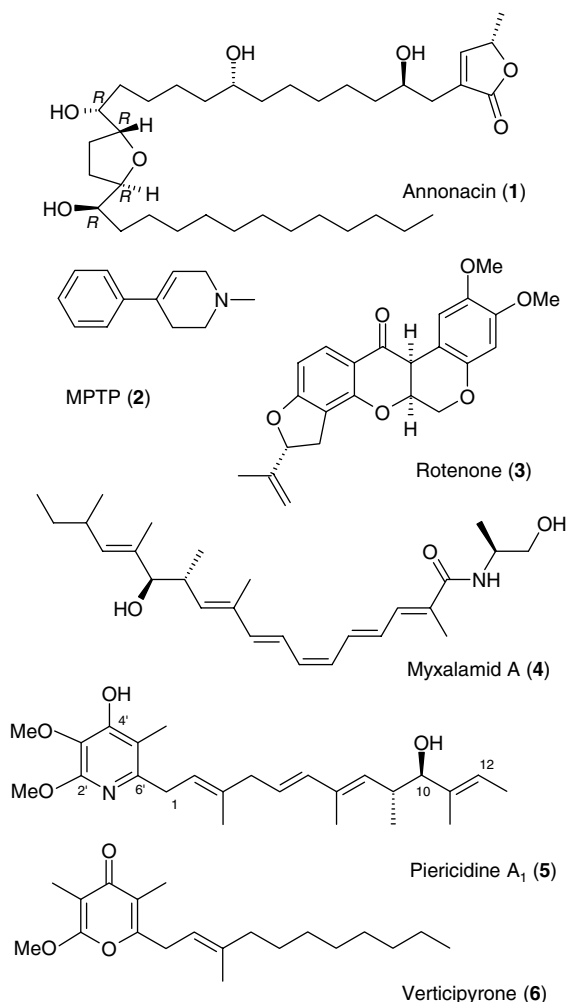
Complex I (NADH-ubiquinone oxidoreductase) is responsible for the first step of the respiratory chain and transfers electrons from NADH to ubiquinone (coenzyme Q). This process is coupled with the transfer

of two protons per electron across the membrane in complex I, which adds to the proton motive force used for ATP synthesis, however, the precise mechanism is mainly unsolved.^{2–4} Complex I is the largest and most complicated enzyme in mammals, for example, bovine heart complex I (M = approx. 1 MDa) consists of 45 subunits, seven of them are encoded by mitochondrial DNA.⁵

For detailed insights in the function and dysfunction of complex I and the affiliated physiological effects, specific inhibitors are used as irreplaceable agents and valuable biochemical tools. This has led to the identification of a number of inhibitors and their use in binding studies,⁶ which already have extensively contributed to the ongoing investigation of the properties of the enzyme and its as yet unsolved dynamic mode of action.⁷ Moreover, several modern pesticides, for example, fenpyroximate, inhibiting complex I have been successfully brought to market.⁸ Presently, inhibitors of complex I are intensely investigated worldwide as exogenous mediators of a wide spectrum of neurodegenerative disorders, including Parkinson's disease or progressive supranuclear palsy.⁹ Thus, the plant-derived annonacin (**1**), a member of

Keywords: Complex I inhibitor; Mitochondrial respiratory chain; Pyridone; *Streptomyces*; Total synthesis.

*Corresponding authors. Tel.: +49 551 393095; fax: +49 551 393228; e-mail addresses: pzezs@gwgdg.de; bku@helmholtz-hzi.de; sgrond@gwdg.de



the acetogenin family, was recently identified as the molecular cause of neurodegenerations (atypical parkinsonism).¹⁰ Synthetic MPTP (1-methyl-4-phenyl-1,2,3,6-tetrahydropyridine, **2**) and the plant-derived rotenone (**3**) are now regularly used in cell cultures and model studies of Parkinson's disease.^{10,11}

The enormous structural diversity of known inhibitors of complex I, which also includes microbial myxalamids (e.g., **4**)¹² and piericidins (e.g., **5**)¹³ as well as the fungal

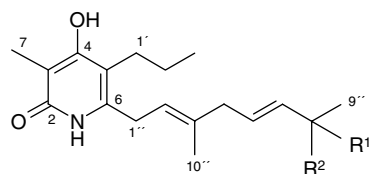
verticipyron (**6**),¹⁴ has led to attempts to classify these compounds into three fundamental types based on their presumed different modes of inhibition in the ubiquinone redox cycle and thus, different binding sites.⁶ However, current hypotheses of the inhibitor binding domain suggest a common large binding pocket, which is constructed by multiple subunits and has several partially overlapping binding positions for the structurally diverse inhibitor molecules. Yet, the understanding of the competitive behavior of established complex I inhibitors is hampered by the possibility that the chemical diverse molecules might either compete for identical binding sites or induce structural dynamic changes in the enzyme which then influence the binding of a second inhibitor.^{15,16}

Recently, we reported about the isolation and total synthesis of iromycins A–D, a unique family of α -pyridone metabolites from *Streptomyces* sp.^{17,18} The striking structural similarities and clear differences with inhibitors **5** and **6** led us to evaluate their inhibitory potential and the site of action within the mitochondrial electron transport chain. Herein, we report on the isolation of the new oxidized metabolites E and F, as well as the synthesis of a variety of derivatives that enabled a comprehensive study on the structure–activity relationships (SAR) of the iromycin family.

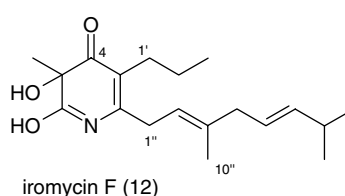
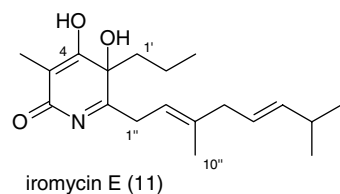
2. Organic and biomolecular chemistry

2.1. Microbial metabolites and semisynthetic derivatives

The iromycins A–D (**7**–**10**) were recently isolated from *Streptomyces bottropensis* sp. Gö Dra 17 in yields of 18 mg/L (**7**), 12 mg/L (**8**), 0.5 mg/L (**9**), and 0.25 mg/L (**10**).¹⁷ With their fully substituted heterocyclic moiety and the long unsaturated side chain, they show distinct similarities with both the ubiquinones as well as verticipyron (**6**), that was lately isolated from the fungus *Verticillium* sp. FKI-1083 as an inhibitor of the NADH fumarate reductase and the complex I.¹⁴ Also structurally related is the piericidin family with about two dozens of compounds. They are produced by different *Streptomyces* strains and belong to the most potent inhibitors of complex I of the mitochondrial electron transport chain.^{13,19}



iromycin	R ¹	R ²
A (7)	CH ₃	H
B (8)	CH ₃	OH
C (9)	H	H
D (10)	H	OH



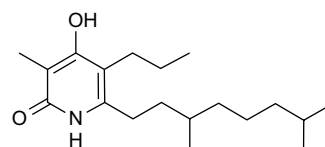
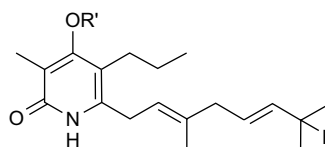
The iromycins **7–10** already revealed a highly interesting biological activity as selective inhibitors of the nitric oxide synthase (NOS) together with an apparent SAR, since iromycin A (**7**) with its terminal isopropyl group is a stronger inhibitor than the hydroxylated derivative B (**8**) or C (**9**) that possesses just a terminal ethyl group. Moreover, it was shown that iromycin B (**8**) is the product of a P450-dependent oxidative degradation of iromycin A (**7**) and thus, iromycin D (**10**) presumably stems from a similar oxidation of iromycin C (**9**).¹⁷ These findings prompted a more detailed search for other oxidized metabolites. Cultivations of the producer strain *Streptomyces* sp. Dra 17 in 10 and 50 L fermenters under the previously reported conditions led to the isolation of two further members of the iromycin family, which were stained violet with anisaldehyde reagent.¹⁷ Iromycin E (**11**) was obtained from the culture filtrate by solid phase extraction (XAD-2, MeOH), silica gel chromatography, gel chromatography (Sephadex LH20), and reverse phase HPLC in an amount of 0.25 mg/L. Iromycin F (**12**) was separated from the fraction mainly containing iromycin A (**7**) by reverse phase HPLC (0.38 mg/L). Structure elucidation was performed using mass spectrometry and NMR methods, and data were compared to that of iromycin A.

Pure iromycin E (**11**) was obtained as a colorless oil and showed low chemical stability even when stored at -20°C . The molecular formula, $\text{C}_{19}\text{H}_{29}\text{NO}_3$, was deduced from the ESI-MS spectrum which showed ions at $m/z = 302$ ($[\text{M}+\text{H}-\text{H}_2\text{O}]^+$) and $m/z = 320$ ($[\text{M}+\text{H}]^+$). It was confirmed by HR-ESI-MS ($m/z = 320.22202$ $[\text{M}+\text{H}]^+$, Δ 0.1 ppm) and points to an oxygenated iromycin derivative. The ^1H NMR spectrum of **11** shows a signal pattern similar to that of iromycin A (**7**) with only few alterations for the unsaturated side chain, for example, with $1''\text{-H}$ shifted upfield to 2.98 ppm. Strong chemical shift differences were observed for the heterocyclic ring system. From the ^{13}C NMR, all signals for the isoprenoid-like side chain (C-6, C-1'' to C10'') were readily identified, however, low signal intensities of the other carbons suggest a dynamic equilibrium, presumably a keto-enol tautomerism, of the molecule in CD_3OD solution. 2D NMR experiments allowed for the assignment of the ^1H and ^{13}C NMR data of the oxygenated pyridone moiety (see [Supplementary Material](#)). Observed key HMBC correlations are $1''\text{-H}$ (δ_{H} 2.98) and $1'\text{-H}$ (δ_{H} 1.59) with C-6 (δ_{C} 177.6), and 7-H (δ_{H} 1.94) with C-3 (δ_{C} 106.1) and C-4 (δ_{C} 165.7) connecting the side chains with the heterocycle, and correspond with the assigned structure **11** for the 5*H*-pyridin-2-one metabolite iromycin E.

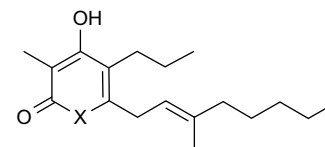
The ESI-MS of iromycin F (**12**), also obtained as a colorless oil, showed an $[\text{M}+\text{H}]^+$ ion at $m/z = 320$ and a $[\text{2M}+\text{Na}]^+$ ion at $m/z = 661$. The molecular formula, $\text{C}_{19}\text{H}_{29}\text{NO}_3$, was determined by HR-ESI-MS ($m/z = 320.22227$ $[\text{M}+\text{H}]^+$, Δ 0.8 ppm). The signal pattern of the NMR spectra of **12** is very similar to both **11** and **7** and suggested a constitutional isomer of **11**. Compared to iromycin A (**7**), the proton NMR spectrum shows significant high field shifts of the signals of

$1''\text{-H}$ to 3.10/3.20 ppm and of 7-H to 1.47 ppm. Striking differences in the carbon NMR spectrum are signals at $\delta_{\text{C}} = 178.1$ ppm, as well as at 199.6 and 79.4 ppm indicating a keto group and a hydroxy group, respectively. The constitution of **12** was fully resolved from 1D and 2D NMR experiments which give evidence for the known $\text{C}_3\text{-}$ and $\text{C}_{10}\text{-side}$ chains, and a new ring structure with an additional hydroxy group at C-3 (see [Supplementary Material](#)). Multiple HMBC correlations of 7-H, $1'\text{-H}$, $1''\text{-H}$, and $10''\text{-H}$ unambiguously determined the structure of the new member of the iromycin family, the 3*H*-pyridin-4-one analogue **12**. Thus, oxygenation of iromycin A (**7**) not only occurs at the isopropyl moiety of the side chain to furnish the known iromycin B (**8**), but also modifies the cyclic moiety of the iromycins to generate the new iromycins E (**11**) and F (**12**).

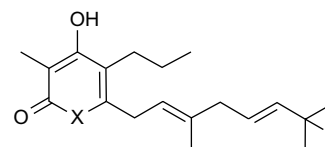
The non-natural derivatives iromycin AH (**13**), AM (**14**), BM (**15**), AA (**16**), and BA (**17**) were prepared from the microbial metabolites iromycin A (**7**) and B (**8**) which can be isolated from *Streptomyces* sp. Dra 17 in reasonable amounts.¹⁷ General protocols for the hydrogenation with H_2 over Pd/C, the methylation with diazomethane, and the acetylation with acetic anhydride were applied.¹⁷ Thus, another five iromycin analogues with chemical changes in the side chain as well as in the heterocyclic core were obtained as pure compounds and used for structural characterization and biological profiling.

iromycin AH (**13**)

iromycin	R	R'
AM (14)	H	Me
BM (15)	OH	Me
AA (16)	H	Ac
BA (17)	OH	Ac



iromycin	X
M (18)	NH
MO (19)	O



iromycin	X	R
S (20)	NH	Me
SO (21)	O	Me
AO (22)	O	H

2.2. Total synthesis

The structural novelty and promising biological activity of the iromycins made their total synthesis an attractive aim. Therefore, a highly convergent access to these com-

pounds was developed, that consists of a coupling of the heterocyclic moiety as a pyrone derivative with the side chains as alkenyl alanates on a late stage of the synthesis and already led to the formation of iromycin A (**7**) in 18% overall yield and non-natural iromycin M (**18**) in 14% overall yield.¹⁸ As the NOS inhibition potential of the iromycins increases with the steric bulk of the end cap of the side chain—which could be the consequence of a higher lipophilicity—the synthesis of the respective *tert*-butyl derivative, iromycin S (**20**), was envisaged and thus of a derivative, which should also resist the degradation by side chain hydroxylation.

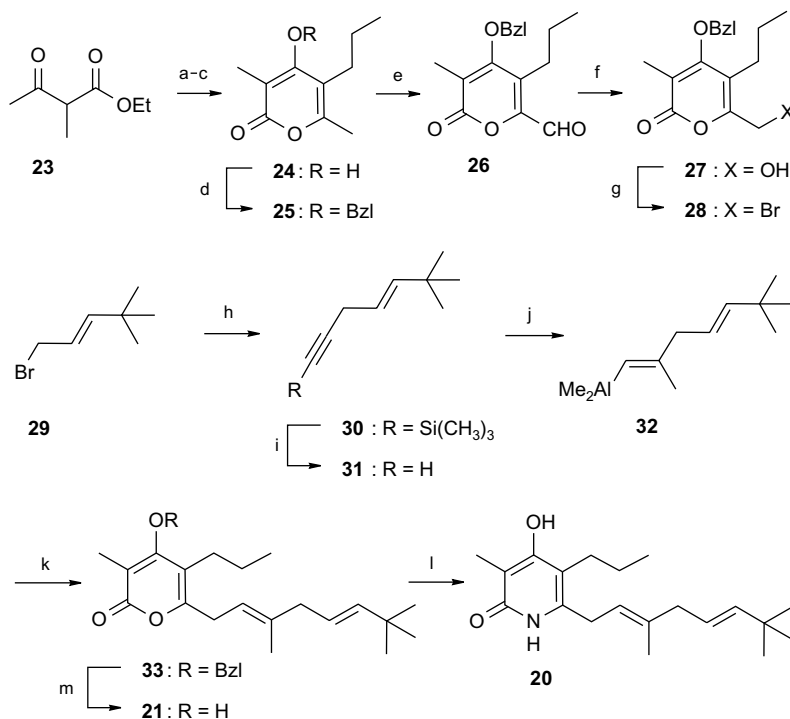
The ring fragment **28** was obtained by propylation, acylation, and cyclization of the β -ketoester **23** and subsequent protection of the hydroxy moiety and functionalization of the 6-methyl group in **24** (Scheme 1).¹⁸ The side chain of iromycin S (**20**) was prepared from bromide **29**, which, in turn, is readily obtainable from pivaldehyde.²⁰ A copper-catalyzed alkynylation furnished enyne **30** which was desilylated and then carboaluminated with AlMe_3 ²¹ to form alkenylalane **32**. Treatment of this compound with *n*BuLi yielded the corresponding lithium trialkylalkenyl alanate which smoothly underwent a cross coupling reaction with the ring fragment **28** to furnish the benzoylated pyrone analogue **33** of iromycin S. This compound was then reacted with liquid ammonia in an autoclave at 70 °C which led to both, formation of the respective pyridone and debenzoylation of the hydroxy moiety to yield iromycin S (**20**) in 14% overall yield. The formation of the iromycins

along this sequence offers the additional advantage of providing the respective O-analogues by simple debenzoylation of the pyrone intermediates instead of their treatment with ammonia. Thus, the pyrone **21** (iromycin SO) was obtained by saponification of compound **33**, and the iromycins MO and AO (**19**, **22**) were formed accordingly.

Table 1. Inhibitory effect of iromycins (**7–22**) on NADH oxidation in bovine heart submitochondrial particles (SMP) in comparison with piericidin A₁ (**5**)

Compound	IC ₅₀ (ng/mL)	IC ₅₀ (μM)
Iromycin A (7)	140	0.461
Iromycin B (8)	5700	17.8
Iromycin C (9)	1020	3.52
Iromycin D (10)	>8097	>26.5
Iromycin E (11)	>8097	>25.3
Iromycin F (12)	>8097	>25.3
Iromycin AH (13)	680	2.21
Iromycin AM (14)	890	2.80
Iromycin BM (15)	>8097	>24.3
Iromycin AA (16)	>8097	>23.4
Iromycin BA (17)	>8097	>22.4
Iromycin M (18)	295	1.01
Iromycin MO (19)	2500	8.55
Iromycin S (20)	58	0.183
Iromycin SO (21)	4800	15.1
Iromycin AO (22)	>8097	>26.6
Piericidin A ₁ (5)	2.1	0.005

The rate of NADH oxidation without inhibitor was $1.1 \pm 0.46 \mu\text{mol mg}^{-1} \text{ min}^{-1}$.



Scheme 1. Total synthesis of iromycins S (**20**) and SO (**21**). Reagents and conditions: (a) LDA (2.2 equiv), THF, 0 °C, 0.5 h, then *n*PrI, 0 °C, 2.5 h; (b) LDA (2.6 equiv), THF, 0 °C, 1 h, then *N*-acetylimidazole, −78 °C, 2 h; (c) DBU, benzene, Δ , 6 h, 36% from **23**; (d) BzlCl, pyridine, rt, 44 h, 89%; (e) SeO₂, dioxane, 130 °C, 16 h, 99%; (f) NaBH₄, EtOH, 0 °C → rt, 4 h, 91%; (g) PBr₃, dioxane, rt, 15 h, 99%; (h) Trimethylsilylacetylene, *n*BuMgBr, THF, 0 °C → rt, 2 h, then CuCN, **29**, −5 °C → rt, 16 h, 90%; (i) NaOH, MeOH/H₂O, rt, 4 h, 82%; (j) Cp₂ZrCl₂, AlMe₃, ClCH₂CH₂Cl, 0 °C → rt, 2 h, 89%; (k) *n*BuLi, THF, 0 °C, 0.5 h, then **28**, 0 °C, 2.5 h, 79%; (l) NH₃(l), 70 °C, 48 h, 63%; (m) NaOH, Dioxan/H₂O, rt, 16 h.

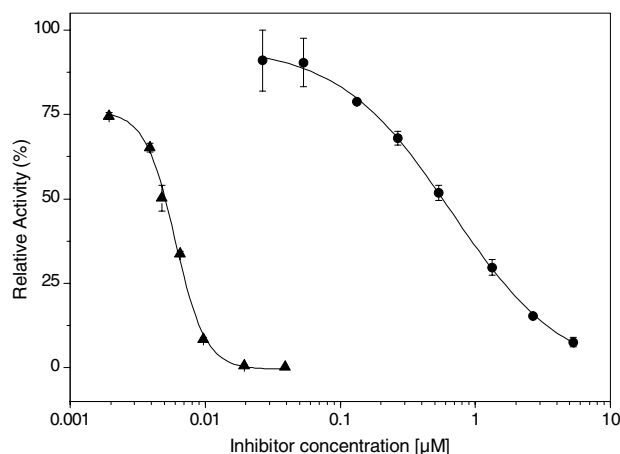


Figure 1. Dose-dependant inhibition of NADH-oxidation in bovine heart submitochondrial particles by iromycin A (**7**, ●) in comparison with piericidin A₁ (**5**, ▲). Values represent means \pm SEM of 2–4 independent experiments, respectively. The rate of NADH oxidation without inhibitor was $1.2 \pm 0.2 \mu\text{mol mg}^{-1} \text{min}^{-1}$.

3. Effects on the mitochondrial electron transport and biological profile

The iromycins and their pyrone analogues **7–22** were investigated for their potential to act as electron transport inhibitors by testing their inhibitory efficacy on NADH oxidation in beef heart submitochondrial particles (SMP) (Table 1 and Fig. 1). Piericidin A₁ (**5**) was included as a control. As anticipated from the structural analogies, some iromycins indeed significantly blocked the mitochondrial electron transport, in particular the natural iromycins **7**, **9**, the semisynthetic **13**, **14** and synthetic agents **18**, **20**.

As shown in Figure 1, iromycin A (**7**) inhibited NADH oxidation half-maximally (IC_{50}) at a concentration of 140 ng/mL (0.461 μM). The IC_{50} value for piericidin A₁ (**5**) in the same test system was 2.1 ng/mL (0.005 μM), which is comparable with the values given in the literature.¹³ Metabolite **7** with its isopropyl group as end cap is sevenfold more potent than **9** ($\text{IC}_{50} = 1020 \text{ ng/mL}$, 3.5 μM) with its less branched side chain. Compared to these, the 7''-hydroxylated metabolites **8** and **10** and the ring oxidized analogues **11** and **12** display no significant inhibitory activity. Hydrogenation and methylation of iromycin A (analogues **13** and **14**) reduces the potency by a factor of 5–6. In contrast, the other semisynthetic derivatives **15–17** as well as the synthetic pyrone intermediates **19**, **21**, and **22** are not active. Remarkably, iromycin M (**18**) resembling a 5'',6''-dihydroanalogue of iromycin C (**9**) is 3.5-fold more potent than the latter. Yet, the most potent of all these congeners is iromycin S (**20**), that carries a more bulky *t*-butyl group in the side chain and is about 2.5-fold more active in the complex I inhibition assay than the natural metabolite **7**.

The site of inhibition of iromycin A within the respiratory chain was investigated by means of difference spectroscopy. Upon reduction with physiological substrates,

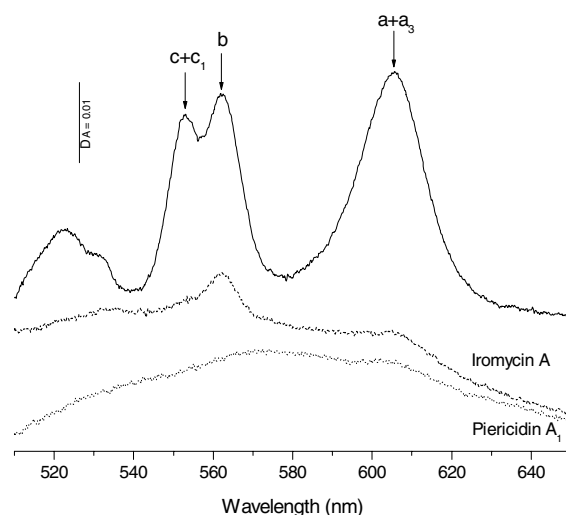


Figure 2. The effect of iromycin A (**7**) in comparison to piericidin A₁ (**5**) on the reduction of cytochromes by NADH. — Difference spectrum (reduced minus oxidized) of SMP reduced with NADH without inhibitor --- in the presence of 30 $\mu\text{g/mL}$ iromycin A, and ... in the presence of 15 $\mu\text{g/mL}$ piericidin A₁.

for example, NADH, fully oxidized cytochromes in front of the block become reduced, while those behind it remain oxidized. The difference spectrum of NADH-reduced minus air-oxidized SMP without inhibitor showed the characteristic absorption maxima for the different cytochromes (Fig. 2). Treatment of SMP with either iromycin A (**7**) or piericidin A₁ (**5**) almost completely inhibited reduction of cytochrome aa₃ (alpha band at 606 nm), cytochrome b (alpha band at 563 nm), and the cytochromes c + c₁ (alpha band at 553 nm) by NADH. These results indicate that the inhibitory effect of iromycin A (**7**), like that of piericidin A₁ (**5**), is mediated via interaction with complex I (NADH-ubiquinone oxidoreductase) of the eukaryotic respiratory chain. However, a more exact determination of the mode of action of iromycins requires further investigation.

No activity was observed for iromycins A (**7**) and B (**8**) in a test panel for herbicide, insecticide, and fungicide activity. To evaluate the cytotoxic potential, compounds **7** and **8** were tested on cancer cell lines HM02 (gastric adenocarcinoma), HepG2 (hepatocellular carcinoma), and MCF7 (breast adenocarcinoma) corresponding NCI-directives, but showed no activity ($\text{IC}_{50} > 10 \mu\text{g/mL}$ ($> 30 \mu\text{M}$)). Moreover, **7** is known to be non-toxic upon intraperitoneal injection in mice (100 mg/kg).²² In addition, we checked the cytotoxicity of **5**, **7**, **8**, **18**, and **20** in parallel, using L929 mouse fibroblasts,²³ and clearly obtained high cytotoxic activity for piericidin A₁ (**5**, IC_{50} 0.18 ng/mL, 0.43 nM), but no or very low effect for the tested iromycins. The IC_{50} for iromycins A (**7**), B (**8**), and M (**18**), respectively, was at about 20 $\mu\text{g/mL}$ (approx. 66 μM) and those of iromycin S (**20**) was at about 3 $\mu\text{g/mL}$ (10 μM). All results demonstrate that even the most potent compound of the iromycin family shows only marginal cytotoxicity in comparison to piericidin A₁ (**5**).

4. Discussion of structure–activity relationships

Isolated as a group of metabolites from *Streptomyces* sp., the piericidins (e.g., **5**) feature the fully substituted 4-hydroxypyridine core as a ‘cyclic head’, together with the branched, unsaturated side chain as a ‘hydrophobic tail’. They have been widely recognized as highly active complex I inhibitors. They exhibit promising biological activity in a broad range as insecticides, antimicrobial or antifungal agents, and also as inhibitors of immune response proteins. Additionally, the highly selective antitumor activity and great potency of certain piericidins prompted a detailed investigation of SAR.^{13,19,24–26} However, the different mechanisms of action have yet not been established, and the high chemical instability and significant cytotoxicity of the piericidins impairs their broad use in biochemical studies.

The iromycins possess similar structural features as the piericidins (e.g., **5**) and verticypyrone (**6**), in particular a heterocyclic core structure and a side chain with a non-conjugated double bond in β,γ -position to the ring. However, the distinct differences between the compounds investigated in this study allow for the discussion of structure–activity relationships with the following points:

(a) The most active iromycin S ($IC_{50} = 0.183 \mu M$) and the natural iromycin A ($IC_{50} = 0.461 \mu M$) are 40- to 90-fold less potent than the known piericidin **5** ($IC_{50} = 0.005 \mu M$). Thus, their lower potency might either originate from the different type of heterocyclic moiety, the longer alkyl substituent at C-5, or the shorter isoprenoid-like side chain.^{25,26} (b) Non-natural **20** with its *t*-butyl moiety presumably contains the most lipophilic side chain, while **8**, **10**, **15**, and **17** are 7''-hydroxylated and show no inhibition on NADH oxidation in SMP ($IC_{50} > 17 \mu M$). In contrast, the highly active piericidin A₁ (**5**) carries a hydroxy group at C-10 of the side chain, but also tolerates its removal as long as the 4-hydroxy pyridine moiety remains unchanged.^{13,24} (c) The β,γ -positioned double bond is an exceptional feature of the cyanobacterial toxic kalkipyrrone²⁷ and the complex I inhibitors such as **5**, **6**, **7**, and **20**. Surprisingly, mono-unsaturated iromycin M (**18**) only containing this double bond is even threefold more active than the natural, bis-unsaturated **9**. While complete hydrogenation of the side chain in piericidins was reported to reduce the potency by a factor of 36,¹⁹ the saturated iromycin AH (**13**) is still more active than **9** and only fivefold less active than its bis-unsaturated homologue **7**. (d) The α -pyrone analogues of the iromycins turned out to be inactive ($IC_{50} > 9 \mu M$), though the γ -pyrone family of the verticypyrone shows strong inhibitory capacity ($IC_{50} > 0.046 \mu M$).¹⁴ (e) As stated for the piericidins, the 4-hydroxy function on the heterocycle is of high importance. This does not apply to additional hydroxy functions on the cyclic head such as in **11** or **12**, abolishing the significant acidity of the 4-OH. In analogy, methylated and acetylated iromycins **14**, **15**, **16**, and **17** show weak or no inhibitory action, respectively. (f) With respect to the modes of action classified by Esposti,⁶ the iromycins might be type B inhibitors,

acting as antagonists of the semiquinone intermediate stabilized within the complex, and thus they could be similar to rotenone and those piericidin derivatives containing a hydroxy group on the ring and a non-hydroxylated side chain. In contrast, natural piericidins also show type A inhibition and act as an ubiquinone competitor.

5. Conclusion

New iromycins have been isolated and synthesized. To determine structure–activity relationships, their efficacy on NADH oxidation in beef heart SMP was tested in comparison to iromycin A (**7**) and piericidin A₁ (**5**). The inhibitory potential of the iromycins is clearly modulated by the structural features discussed here and shows analogies with the piericidins. However, some pronounced differences between both metabolite families were stated. It was already recognized that the cytotoxicity of different piericidin congeners does not necessarily correlate with their respective complex I inhibition.¹³ Thus, the marginal cytotoxicity of the iromycins paired with a significant complex I inhibition provides another hint, that additional effects than just blocking of the electron transport chain might cause the high toxicity of the piericidins. Moreover, a vasodilating activity was noted for some piericidins,²⁸ while the iromycins are presumably vasoconstrictors due to their inhibition of the NOS.¹⁷ Clearly, more detailed investigations are necessary to both, broadly evaluate and then understand the biological profile of these *Streptomyces* metabolites. This includes competitive binding studies of the iromycins and known inhibitors. With the established total synthesis at hand, we are now working towards the preparation of hybrids of the iromycins and piericidins, and additional analogues should be obtained from precursor-directed biosynthesis.

Altogether, the new iromycin family sets the stage for the identification of potent but non-cytotoxic complex I inhibitors which would be ideal biochemical tools not only for the investigation of the complex I enzyme, but also for pharmacologically relevant studies on neurodegenerative diseases.

6. Experimental

6.1. General experimental methods

Fermentations, extractions, and column chromatography were performed as described elsewhere.¹⁷ For special equipment and solvents, see [Supplementary Material](#). HPLC: pump Jasco PU-1587; detector Jasco UV/VIS 1575; software Jasco-Borwin 1.50; preparative HPLC conditions: column A: Machery & Nagel Nucleodur 100-5 C18 ec. (250 × 8 mm), flow rate: 2.5 mL min⁻¹; column B: Grom, Supersphere 100 C18 ec. (4 μ m, 100 × 8 mm), flow rate 2.5 mL min⁻¹; column C: Grom, Supersphere 100 C18 ec. (4 μ m, 100 × 20 mm), flow rate 14 mL min⁻¹; HPLC programs: Solution A: H₂O, solution B: acetonitrile, solution C: MeOH; program A:

40% A to 100% C in 25 min, 5 min 100% C; program B: 55% A to 100% C in 25 min, 5 min 100% C. Iromycin E (**11**): isocratic 30% B, 70% A, column A. Iromycin F (**12**): isocratic 60% B, 40% A, column A. Iromycin AH (**13**), AM (**14**), BM (**15**), AA (**16**): program A, column B. Iromycin BA (**17**): program B, column B. Butyl lithium was titrated according to the method of Suffert.²⁹ THF and hexane were distilled from sodium benzophenone ketyl, 1,2-dichloroethane was distilled from CaH₂. Iromycins AM (**14**) and AA (**16**),¹⁷ iromycin M (**18**) and 4-benzoyloxy-6-bromomethyl-3-methyl-5-propylpyran-2-one (**28**),¹⁸ and (*E*)-1-bromo-4,4-dimethylpent-2-ene (**29**)²⁰ were prepared as described in the literature.

6.2. Mitochondrial preparations

Submitochondrial particles (SMP) of bovine heart were obtained by ultrasonic treatment of the mitochondria, which were isolated by differential centrifugation, following the protocol of Smith by using a blender to homogenize the heart mince.³⁰ The initial homogenization buffer consisted of 250 mM sucrose, 10 mM KH₂PO₄, 10 mM Tris, 2 mM EGTA, 2 mM MgCl₂, pH 7.4. Further isolation procedures were carried out in the same medium without EGTA.³¹

6.3. Measurements of NADH-oxidation and difference spectra

In both assays, SMP were suspended in 75 mM air saturated sodium potassium phosphate buffer, pH 7.4, with 1 mM each of EDTA and MgCl₂. The test compounds were added in methanolic solution to the reaction chamber and the methanol concentration in all tests did not exceed 2% (v/v).

The tests were performed at 30 °C and contained in the different sample preparations 42–219 µg/mL of bovine protein. After 4 min of preincubation at 30 °C with or without inhibitors, the reaction was started by the addition of NADH to give a final concentration of 0.16 mM. The rate of NADH oxidation was measured within 4 min as a decrease in optical density at 340 nm in a UV2 Unicam UV/VIS spectrophotometer. Difference spectra of NADH-reduced minus air-oxidized were recorded at room temperature in a DW-2000 UV/VIS SLM Aminco double-beam spectrophotometer (American Instruments, Silver Springs, MD, USA). The SMP were suspended to give a final concentration of 2.35 mg protein/mL. The preincubation with or without inhibitors in the sample cuvette was performed for 2 min and the reduction of SMP in the sample cuvette was carried out by the addition of NADH (final concentration 2 mM). The bandwidth was 2 nm and the speed 1 nm/s.

6.4. Iromycin E (4,5-dihydroxy-6-[(*E,E*)-(3,7-dimethylocta-2,5-dienyl)-3-methyl-5-propyl-5*H*-pyridin-2-one, **11**)

Total amount of isolated metabolite: 2.5 mg. C₁₉H₂₉NO₃ (*M_r* = 319.45); ESI-MS: *m/z* = 302 [M+H–H₂O]⁺, 320 [M+H]⁺, 342 [M+Na]⁺, 661 [2M+Na]⁺; HR-ESI-MS: Found: 320.22200, calculated for C₁₉H₃₀NO₃ 320.22202 (Δ 0.06 ppm); [α]_D²⁰ = –380° (*c* = 1.0, MeOH); IR (KBr):

ν 3421, 2959, 2929, 1718, 1636, 1560, 1458, 1380, 1050 cm^{–1}; UV (MeOH): λ_{max} nm (*ε*): 279 (278), 203 (2526); UV (MeOH+NaOH): λ_{max} nm (*ε*): 278 (197), 220 (749); *R_f*-values: 0.73 (cyclohexane/EtOAc/MeOH 5:10:2), 0.49 (MeOH/H₂O 7:3); ¹H NMR (300 MHz, CD₃OD): δ 0.89 (m, 3H, 3'-H₃), 0.96 (d, *J* = 7.0 Hz, 6H, 8''-H₃, 9''-H₃), 1.24 (m, 2H, 2'-H₂), 1.94 (s, 3H, 7-H₃), 1.59 (s, 3H, 10''-H₃), 2.26 (m, 1H, 7''-H), 1.59/2.26 (m, 2H, 1'-H_a/1'-H_b), 2.66 (d, *J* = 6.5 Hz, 2H, 4''-H₂), 2.98 (d, *J* = 7.0 Hz, 2H, 1''-H₂), 5.35 (m, 1H, 2''-H), 5.34 (m, 1H, 5''-H), 5.40 (m, *J* = 15.5 Hz, 1H, 6''-H) ppm; ¹³C NMR (75.5 MHz, CD₃OD): δ 8.6 (+, C-7), 14.3 (+, C-3'), 16.1 (+, C-10''), 22.9 (+, C-8'', C-9''), 27.8 (–, C-1'), 30.4 (–, C-2'), 32.3 (+, C-7''), 35.1 (–, C-1''), 43.8 (–, C-4''), 71.0 (C_{quat}, C-5), 106.1 (C_{quat}, C-3), 118.8 (+, C-2''), 126.1 (+, C-5''), 138.2 (C_{quat}, C-3''), 140.3 (+, C-6''), 165.7 (C_{quat}, C-4), 176.6 (C_{quat}, C-2), 177.6 (C_{quat}, C-6) ppm.

6.5. Iromycin F (2,3-dihydroxy-6-[(*E,E*)-(3,7-dimethylocta-2,5-dienyl)-3-methyl-5-propyl-3*H*-pyridin-4-one, **12**)

Total amount of isolated metabolite: 3.8 mg. C₁₉H₂₉NO₃ (*M_r* = 319.45); ESI-MS: *m/z* = 320 [M+H]⁺, 342 [M+Na]⁺, 661 [2M+Na]⁺; HR-ESI-MS: Found: 320.22227, calculated for C₁₉H₃₀NO₃ 320.22202 (Δ 0.8 ppm); [α]_D²⁰ = –23° (*c* = 1.0, MeOH); IR (KBr): *ν* 3420, 2962, 2933, 2873, 1716, 1662, 1624, 1458, 1384, 1196, 1116, 1062 cm^{–1}; UV (MeOH): λ_{max} nm (*ε*): 312 (1561), 202 (3818); UV (MeOH+NaOH): λ_{max} nm (*ε*): 316 (1295), 206 (3056); *R_f*-values: 0.25 (CHCl₃/MeOH 9:1), 0.74 (cyclohexane/EtOAc/MeOH 5:10:2), 0.24 (MeOH/H₂O 7:3); ¹H NMR (300 MHz, CD₃OD): δ 0.91 (t, *J* = 7.0 Hz, 3H, 3'-H₃), 0.96 (d, *J* = 7.0 Hz, 6H, 8''-H₃, 9''-H₃), 1.38 (m, *J* = 7.0 Hz, 2H, 2'-H₂), 1.47 (s, 3H, 7-H₃), 1.71 (s, 3H, 10''-H₃), 2.24 (m, 1H, 7''-H), 2.10–2.40 (m, 2H, 1'-H₂), 2.69 (d, *J* = 6.5 Hz, 2H, 4''-H₂), 3.10 (m, *J* = 16.0, 7.0 Hz, 1H, 1''-H_a), 3.20 (m, *J* = 16.0, 7.0 Hz, 1H, 1''-H_b), 5.16 (m, *J* = 7.0 Hz, 1H, 2''-H), 5.35 (m, *J* = 15.5, 6.5 Hz, 1H, 5''-H), 5.40 (m, *J* = 15.5, 6.5 Hz, 1H, 6''-H) ppm; ¹³C NMR (75.5 MHz, CD₃OD): δ 14.4 (+, C-3'), 16.7 (+, C-10''), 23.0 (+, C-8'', C-9''), 23.8 (–, C-2'), 27.5 (–, C-1'), 29.2 (+, C-7), 31.3 (–, C-1''), 32.3 (+, C-7''), 43.6 (–, C-4''), 79.4 (C_{quat}, C-3), 114.9 (C_{quat}, C-5), 119.2 (+, C-2''), 125.6 (+, C-5''), 140.1 (C_{quat}, C-3''), 140.9 (+, C-6''), 154.4 (C_{quat}, C-6), 178.1 (C_{quat}, C-2), 199.6 (C_{quat}, C-4) ppm.

6.6. Iromycin AH (6-(3,7-dimethyloctanyl)-4-hydroxy-3-methyl-5-propyl-1*H*-pyridin-2-one, **13**)

Iromycin A (**7**, 41.7 mg, 0.137 mmol) was dissolved in CH₃OH (10 mL) and Pd/C (20 mg) was added to the stirred solution under H₂ atmosphere. After 2 h the suspension was filtered, and evaporation of the solvents gave the crude product which was purified using preparative HPLC (column C, program A) to yield 5.8 mg (14%) of pure compound **13**. C₁₉H₃₃NO₂ (*M_r* = 307.48); ESI-MS: *m/z* = 308 [M+H]⁺; IR (KBr): *ν* 3421, 2963 (sh), 2873, 1654, 1560, 1547, 1375, 1167 cm^{–1}; UV (MeOH): λ_{max} nm (*ε*): 209 (4192), 287 (1051); UV (MeOH+NaOH): λ_{max} nm (*ε*): 204 (6564), 217 (4343), 274 (1030). *R_f*-values: 0.10

(CHCl₃/MeOH 9:1), 0.52 (cyclohexane/EtOAc/MeOH 5:10:2), 0.77 (MeOH/H₂O 7:3); ¹H NMR (300 MHz, CD₃OD): δ 0.88 (d, *J* = 7.0 Hz, 6H, 8''-H₃, 9''-H₃), 0.95 (m, 3H, 10''-H₃), 0.96 (m, *J* = 7.0 Hz, 3H, 3'-H₃), 1.14–1.20 (m, 3 H, 4''-H_a, 6''-H₂), 1.28–1.41 (m, 4 H, 2''-H_a, 4''-H_b, 5''-H₂), 1.47–1.61 (m, 5H, 2'-H₂, 2''-H_b, 3''-H, 7''-H), 1.95 (s, 3H, 7-H₃), 2.42 (m, 2H, 1'-H₂), 2.47–2.59 (m, 2H, 1''-H₂) ppm; ¹³C NMR (75.5 MHz, CD₃OD): δ 8.7 (+, C-7), 14.5 (+, C-3'), 19.9 (+, C-10''), 23.0 (+, C-8'', C-9''), 24.4 (–, C-2'), 25.9 (–, C-5''), 28.0 (–, C-1'), 29.0 (–, C-1''), 29.2 (+, C-7''), 34.2 (–, C-3''), 38.1 (–, C-2''), 38.1 (–, C-4''), 40.4 (+, C-6''), 105.8 (C_{quat}, C-3), 113.3 (C_{quat}, C-5), 144.7 (C_{quat}, C-6), 166.0 (C_{quat}, C-2), 166.3 (C_{quat}, C-4) ppm.

Iromycin AM (**14**), BM (**15**), AA (**16**), and BA (**17**) were prepared according to the known procedures and the experimental details of **14** and **16** are described elsewhere.¹⁷ See [Supplementary Material](#) for the characterization data of **15** and **17**.

6.7. (*E*)-6,6-Dimethyl-1-trimethylsilylhept-4-en-1-yne (**30**)

n-Butylmagnesium bromide (22 mL, 35 mmol, 1.6 M in Et₂O) was added dropwise at 0 °C to a solution of trimethylsilylacetylene (5.05 mL, 3.51 g, 35.7 mmol) in THF (40 mL), and the mixture was stirred for 2 h at rt. The thus obtained trimethylsilylthynylmagnesium bromide was transferred by cannula to a precooled (–5 °C) mixture of (*E*)-1-bromo-4,4-dimethylpent-2-ene (**29**) (4.165 g, 23.52 mmol) and CuCN (0.11 g, 1.2 mmol) in THF (50 mL), and the mixture was stirred for 16 h at rt. The reaction mixture was poured into saturated NH₄Cl solution and extracted with Et₂O (3 × 100 mL). The combined organic phases were dried over Na₂SO₄, then filtered, and concentrated in vacuo (100 mbar). The residue was purified by Kugelrohr distillation (70 °C oven temperature, 12 mbar) to yield 4.11 g (90%) of compound **30** as a colorless liquid. C₁₂H₂₂Si (*M*_r = 194.39); EI-MS: *m/z* (%) = 194 (1) [*M*⁺], 179 (3) [*M*⁺–CH₃], 153 (13), 137 (9) [*M*⁺–C₄H₉], 125 (3), 109 (3), 83 (11), 73 (37) [SiMe₃⁺], 57 (100) [C₄H₉⁺]; IR (film): ν 2960, 2177, 1464, 1363, 1250, 971, 842, 760 cm^{–1}; ¹H NMR (250 MHz, CDCl₃): δ 0.19 (s, 9H), 1.00 (s, 9H), 2.95 (dd, *J* = 1.1, *J* = 6.6 Hz, 2H), 5.28 (dt, *J* = 15.5, *J* = 6.6 Hz, 1H), 5.67 (dt, *J* = 15.5, *J* = 1.1 Hz, 1H) ppm; ¹³C NMR (62.9 MHz, CDCl₃, DEPT): δ 0.1(+), 23.0(–), 29.5(+), 32.8 (C_{quat}), 86.0 (C_{quat}), 104.9 (C_{quat}), 118.4(+), 143.1(+) ppm.

6.8. (*E*)-6,6-Dimethylhept-4-en-1-yne (**31**)

NaOH (40 mL, 40 mmol, 1.0 M in H₂O) was added at rt to a solution of silylalkyne **30** (4.54 g, 23.4 mmol) in MeOH (80 mL), and the mixture was stirred for 4 h, poured into saturated NH₄Cl solution, and extracted with pentane (4 × 40 mL). The combined organic phases were dried over MgSO₄, then filtered, and concentrated by careful distillation at atmospheric pressure using a 20 cm Vigreux column. The residue was purified by Kugelrohr distillation (70 °C, 65 mbar) to yield 2.34 g (82%) of enyne **31** as a colorless liquid. C₉H₁₄ (*M*_r = 122.21); EI-MS: *m/z* (%) = 121 (7) [*M*⁺–H], 108

(10), 93 (10), 81 (17), 57 (100) [C₄H₉⁺], 41 (39); IR (film): ν 3309, 2960, 2872, 2120, 1478, 1464, 1364, 1260, 972, 846, 635 cm^{–1}; ¹H NMR (250 MHz, CDCl₃): δ 1.01 (s, 9H), 2.08 (t, *J* = 2.8 Hz, 1H), 2.95 (m_c, 2H), 5.31 (dt, *J* = 15.6, *J* = 5.5 Hz, 1H), 5.68 (dt, *J* = 15.6, *J* = 1.5 Hz, 1H) ppm; ¹³C NMR (62.9 MHz, CDCl₃, DEPT): δ 21.6(–), 29.5(+), 32.8 (C_{quat}), 69.7(+), 82.3 (C_{quat}), 118.2(+), 143.3(+) ppm.

6.9. (*E,E*)-2,6,6-Trimethylhepta-1,4-dienyldimethylalane (**32**)

Cp₂ZrCl₂ (0.274 g, 0.937 mmol) was treated at 0 °C with AlMe₃ (4.68 mL, 9.4 mmol, 2.0 M in hexane, *Caution: pyrophoric!*), and the solvent was removed in vacuo. 1,2-Dichloroethane (5 mL) was added, and the solution was stirred for 30 min at 0 °C. A solution of enyne **31** (0.572 g, 4.68 mmol) in 1,2-dichloroethane (10 mL) was added dropwise, and the mixture was stirred for 2 h at rt. At this point, GC analysis of a hydrolyzed aliquot showed complete consumption of the enyne. The solvent and the excess of AlMe₃ were removed in vacuo, and hexane (1 mL) was added at 0 °C to precipitate the zirconium salts. The mixture was filtered through a frit and the solids were washed with hexane (1 mL). The filtrate was concentrated in vacuo to furnish 0.81 g (89%) of alane **32** as a yellow oil whose purity was >95% as determined by GC analysis of a hydrolyzed aliquot. ¹H NMR (250 MHz, CDCl₃): δ –0.79 (s, 6H), 1.01 (s, 9 H), 2.01 (s, 3H), 2.95 (d, *J* = 5.0 Hz, 2H), 5.24–5.60 (m, 3H) ppm.

6.10. 4-Benzoyloxy-3-methyl-5-propyl-6-[(*E,E*)-3,7,7-trimethylocta-2,5-dienyl]pyran-2-one (**33**)

*n*BuLi (0.35 mL, 0.81 mmol, 2.3 M in hexane) was added to a solution of alane **32** (2.4 mL, 1.2 mmol, 0.50 M in hexane) in THF (1.0 mL) at 0 °C, and the mixture was stirred for 30 min. A solution of 4-benzoyloxy-6-bromo-3-methyl-5-propylpyran-2-one (**28**) (150.0 mg, 0.411 mmol) in THF (2.0 mL) was slowly added at 0 °C, and stirring was continued for 2.5 h. The reaction mixture was poured into saturated NH₄Cl solution (3 mL) and extracted with EtOAc (3 × 15 mL). The combined organic phases were dried over MgSO₄, then filtered, and concentrated in vacuo. The residue was purified by flash column chromatography on SiO₂ (10 g, hexane/EtOAc 6:1) to yield 137 mg (79%) of pyrone **33** (*R*_f = 0.45) as a colorless oil. C₂₇H₃₄O₄ (*M*_r = 422.56); ESI-MS: *m/z* (%) = 423 (100) [*M*+H]⁺, 846 (41) [2*M*+H]⁺; HR-ESI-MS: Found: 423.25326, calculated for C₂₇H₃₅O₄ 423.25299 (Δ 0.6 ppm); IR (film): ν 2959, 1747, 1718, 1577, 1452, 1363, 1243, 1175, 1107, 1063, 1022, 973, 706 cm^{–1}; ¹H NMR (250 MHz, CDCl₃): δ 0.87 (t, *J* = 7.4 Hz, 3H), 1.00 (s, 9H), 1.47 (m_c, 2H), 1.68 (s, 3H), 1.95 (s, 3H), 2.23 (m_c, 2H), 2.67 (d, *J* = 7.3 Hz, 2H), 3.30 (d, *J* = 7.5 Hz, 2H), 5.20–5.31 (m, 2H), 5.48 (d, *J* = 15.5 Hz, 1H), 7.56 (t, *J* = 7.1 Hz, 2H), 7.70 (m_c, 1H), 8.18 (m_c, 2H) ppm; ¹³C NMR (75.5 MHz, CDCl₃, APT): δ 10.5(+), 14.3(+), 16.5(+), 24.2(–), 28.3(–), 30.2(+), 31.1(–), 33.7(–), 43.8(–), 114.3(–), 114.4(–), 119.4(+), 123.3(+), 129.0(–), 130.3(+), 131.3(+), 135.8(+), 139.5(–), 144.7(+), 160.4(–), 161.5(–), 163.8(–), 166.3(–) ppm.

6.11. Iromycin S (4-hydroxy-3-methyl-5-propyl-6-[(E,E)-3,7,7-trimethylocta-2,5-dienyl]-1H-pyridin-2-one, 20)

In an autoclave a mixture of pyrone **33** (61.7 mg, 0.146 mmol) and liquid NH₃ (15 mL) was stirred for 48 h at 70 °C. After the mixture was cooled to rt, the NH₃ was carefully evaporated and the residue was diluted with KHSO₄ solution (1.0 M, 3 mL) and extracted with Et₂O (3 × 20 mL). The combined organic phases were dried over Na₂SO₄, then filtered, and concentrated in vacuo. The residue was purified by flash column chromatography on SiO₂ (8 g, hexane/EtOAc 2:1+1% HOAc) to yield 29.1 mg (63%) of pyridone **20** (*R*_f = 0.33) as a colorless oil. C₂₀H₃₁NO₂ (*M*_r = 317.47); ESI-MS: *m/z* (%) = 340 (10) [M+Na]⁺, 657 (100) [2M+Na]⁺; HR-ESI-MS: Found: 318.24282, calculated for C₂₀H₃₂NO₂ 318.24276 (Δ 0.2 ppm); IR (KBr): ν 2958, 1627, 1456, 1362, 1218, 1163, 1113, 1029, 972 cm⁻¹; ¹H NMR (300 MHz, CD₃OD): δ 0.94 (t, *J* = 7.0 Hz, 3H), 0.99 (s, 9H), 1.47 (m_c, 2H), 1.70 (s, 3 H), 1.98 (s, 3H), 2.40 (m_c, 2H), 2.65 (d, *J* = 7.0 Hz, 2 H), 3.28 (m_c, 2H), 5.15 (t, *J* = 7.0 Hz, 1H), 5.28 (dt, *J* = 15.5, *J* = 7.0 Hz, 1H), 5.47 (d, *J* = 15.5 Hz, 1H) ppm; ¹³C NMR (75.5 MHz, CD₃OD, APT): δ 8.7(+), 14.6(+), 16.5(+), 24.1(–), 28.0(–), 30.1(+), 30.4(–), 33.7(–), 43.8(–), 106.0(–), 113.7(–), 121.1(+), 123.4(+), 138.7(–), 143.0(–), 144.7(+), 165.96(–), 165.99(–) ppm.

6.12. Iromycin MO (19), SO (21), and AO (22)

The respective 4-benzoyloxy-3-methyl-6-(octa-2-enyl)-5-propylpyran-2-one derivative (50 μmol) was dissolved in a solution of NaOH (0.5 M in dioxane/water 1:1, 1.5 mL) and stirred for 16 h at rt. The solution was carefully acidified with hydrochloric acid (1 N) to approx. pH 2 and extracted with EtOAc (3 × 15 mL). The extracts were dried over Na₂SO₄, then filtered, and concentrated in vacuo. The crude product was purified by column chromatography on silica gel to furnish the respective 4-hydroxy-3-methyl-6-(octa-2-enyl)-5-propylpyran-2-one derivatives. See [Supplementary Material](#) for characterization data.

Acknowledgments

This work was financially supported by the Bundesministerium für Bildung und Forschung (GenoMik+: MetabolitGenoMik) and the Deutsche Forschungsgemeinschaft (SFB 416). The authors are indebted to H.J. Langer for valuable discussions and technical assistance. We thank B. Engelhardt for her technical assistance and J. Reinheimer/BASF AG, W. Beil/Hannover Medical University, and F. Sasse/Braunschweig Helmholtz Centre for Infection Research for conducting biological profiling tests. S.G. and P.v.Z. are grateful to Prof. Axel Zeeck and Prof. Armin de Meijere, respectively, for their continuing support.

Supplementary data

Supplementary data associated with this article can be found, in the online version, at [doi:10.1016/j.bmc.2007.11.023](https://doi.org/10.1016/j.bmc.2007.11.023).

References and notes

- Nelson, D. L.; Cox, M. M. *Lehninger Principles of Biochemistry*; Worth: New York, 2000, Chapter 19.
- Yagi, T.; Matsuno-Yagi, A. *Biochemistry* **2003**, *42*, 2266–2274.
- Hirst, J. *Biochem. Soc. Trans.* **2005**, *33*, 525–529.
- Sherwood, S.; Hirst, J. *Biochem. J.* **2006**, *400*, 541–550.
- Carroll, J.; Fearnley, I. M.; Skehel, J. M.; Shannon, R. J.; Hirst, J.; Walker, J. E. *J. Biol. Chem.* **2006**, *281*, 32724–32727.
- (a) Eposti, M. D. *Biochim. Biophys. Acta* **1998**, *1364*, 222–235; (b) Eposti, M. D.; Ghelli, A. *Biochem. Soc. Trans.* **1999**, *27*, 606–609.
- Yamashita, T.; Nakamaru-Ogiso, E.; Miyoshi, H.; Matsuno-Yagi, A.; Yagi, T. *J. Biol. Chem.* **2007**, *282*, 6012–6020.
- Lümmen, P. *Biochim. Biophys. Acta* **1998**, *1364*, 287–296.
- Dauer, W.; Kholodilov, N.; Vila, M.; Trillat, A.-C.; Goodchild, R.; Larsen, K. E.; Staal, R.; Tieu, K.; Schmitz, Y.; Yuan, C. A.; Rocha, M.; Jackson-Lewis, V.; Hersch, S.; Sulzer, D.; Przedborski, S.; Burke, R.; Hen, R. *Proc. Natl. Acad. Sci. U.S.A.* **2002**, *99*, 14524–14529.
- Lannuzel, A.; Michel, P. P.; Höglinger, G. U.; Champy, P.; Jousset, A.; Medja, F.; Lombes, A.; Darios, F.; Gleye, C.; Laurens, A.; Hocquemiller, R.; Hisch, E. C.; Ruberg, M. *Neuroscience* **2003**, *121*, 287–296.
- Perier, C.; Bove, J.; Wu, D.-C.; Dehay, B.; Choi, D.-K.; Jackson-Lewis, V.; Rathke-Hartlieb, S.; Bouillet, P.; Strasser, A.; Schulz, J. B.; Przedborski, S.; Vila, M. *Proc. Natl. Acad. Sci. U.S.A.* **2007**, *104*, 8161–8166.
- Beyer, S.; Kunze, B.; Silakowski, B.; Müller, R. *Biochim. Biophys. Acta* **1999**, *1445*, 185–195.
- Schneermann, M. J.; Romero, F. A.; Hwang, I.; Nakamaru-Ogiso, E.; Yagi, T.; Boger, D. L. *J. Am. Chem. Soc.* **2006**, *128*, 11799–11807.
- Ui, H.; Shiomi, K.; Suzuki, H.; Hatano, H.; Morimoto, H.; Yamaguchi, Y.; Masuma, R.; Sunazuka, T.; Shimamura, H.; Sakamoto, K.; Kita, K.; Miyoshi, H.; Tomoda, H.; Omura, S. *J. Antibiot.* **2006**, *59*, 785–790.
- Murai, M.; Ishihara, A.; Nishioka, T.; Yagi, T.; Miyoshi, H. *Biochemistry* **2007**, *46*, 6409–6416.
- Okun, J. G.; Lümmen, P.; Brandt, U. *J. Biol. Chem.* **1999**, *274*, 2625–2630.
- Surup, F.; Wagner, O.; von Frieling, J.; Schleicher, M.; Oess, S.; Müller, P.; Grond, S. *J. Org. Chem.* **2007**, *72*, 5085–5090.
- Shojaei, H.; Li-Böhmer, Z.; von Zezschwitz, P. *J. Org. Chem.* **2007**, *72*, 5091–5097.
- Yoshida, S.; Takahashi, N. *Heterocycles* **1978**, *10*, 425–467.
- Hoffmann, R. W.; Brinkmann, H.; Frenking, G. *Chem. Ber.* **1990**, *123*, 2387–2394.
- Negishi, E.-i.; Van Horn, D. E.; Yoshida, T. *J. Am. Chem. Soc.* **1985**, *107*, 6639–6647.
- Sukenaga, Y.; Yamazaki, T.; Aoyama, T.; Takayasu, Y.; Harada, T. Japan Patent JP10 237044, 1998, *Chem. Abstr.* **1998**, *129*, 244203S.
- Mosmann, T. *J. Immunol. Meth.* **1983**, *65*, 55–63.
- Gutman, M.; Kliatchko, S. *FEBS Lett.* **1976**, *67*, 348–353.
- Chung, K. H.; Cho, K. Y. *Z. Naturforsch.* **1989**, *44c*, 609–616.
- Yoshida, S.; Nagao, Y.; Watanabe, A.; Takahashi, N. *Agric. Biol. Chem.* **1980**, *44*, 2921–2924.
- Graber, G. M.; Gerwick, W. H. *J. Nat. Prod.* **1998**, *61*, 677–680.
- Kominato, K.; Watanabe, Y.; Hirano, S.-I.; Kioka, T.; Terasawa, T.; Yoshioka, T.; Okamura, K.; Tone, H. *J. Antibiot.* **1995**, *48*, 99–102, 103–105.
- Suffert, J. *J. Org. Chem.* **1989**, *54*, 509–510.
- Smith, A. L. *Methods Enzymol.* **1967**, *10*, 81–86.
- Thierbach, G.; Reichenbach, H. *Biochim. Biophys. Acta* **1981**, *638*, 282–289.